Anti-corrosion Properties of Rosemary Oil and Vanillin on Low Carbon Steel in Dilute Acid Solutions

Roland Tolulope Loto, Cleophas Akintoye Loto, Bryan Ayozie and Tayo Sanni

Abstract The corrosion inhibition effect of rosemary oil and vanillin (ROV) on low carbon steel in 1 M HCl and H_2SO_4 media was studied through potentiodynamic polarization, weight loss analysis, optical microscopy and IR spectroscopy. Results showed optimal inhibition performance of the compound, but more effectively in HCl solution at 92.57 and 94% compared to 64.57 and 64.55% in H_2SO_4 from both electrochemical test. Identified functional groups of the admixture from IR spectroscopy completely adsorbed on the steel in HCl, but partially in H_2SO_4. Thermodynamic calculations showed chemisorption and physiochemical adsorption according to Langmuir, Freundlich and Temkin isotherm model. Micro-analytical images revealed a well-protected ROV inhibited steel surface in comparison to images from the corroded stainless steel. The inhibition behavior of ROV was determined to be mixed type.

Keywords Corrosion · Inhibitor · Rosemary oil · Vanillin
Acid

Introduction

Corrosion inhibition by chemical compounds is of great practical importance, being extensively employed in curtailing wastage of engineering materials and minimizing costs of corrosion control. The use of inhibitors is quite varied often playing an important role in oil extraction and processing industries, heavy industrial manufacturing, water treatment facility etc. to minimize localized corrosion and

R. T. Loto (✉) · C. A. Loto · B. Ayozie
Department of Mechanical Engineering, Covenant University,
Ota, Ogun State, Nigeria
e-mail: tolu.loto@gmail.com

T. Sanni
Department of Chemical, Metallurgical and Materials Engineering,
Tshwane University of Technology, Pretoria, South Africa

unexpected sudden failures. The effectiveness or corrosion inhibition efficiency of a corrosion inhibitor is a function of many factors, including but not limited to fluid composition, mixability water, presence of heteroatoms, molecular structure, flow regime and strength of adsorption with the steel surface. Molecules of natural or organic origin exhibiting a strong affinity for metallic surfaces is the focus of this research toward the development of environmentally tolerant corrosion inhibiting compounds.

Experimental Methods

Low carbon steel (LCS) with a nominal composition 0.8% Mn, 0.04% P, 0.05% S, 0.16% C and 98.95% Fe is the steel test specimen in cylindrical form with dimensions of length, 1 cm and diameter, 1 cm after machining and metallographic preparation. Vanillin and rosemary oil obtained are the organic compounds evaluated for their synergistic corrosion inhibiting properties in combined molar concentrations of 2.96×10^{-3}, 5.93×10^{-2}, 8.89×10^{-2}, 1.19×10^{-2}, 1.48×10^{-2}, 1.78×1^{-2}, in 200 mL of 1 M HCl and H_2SO_4 acid solutions. Polarization measurements were carried out at 30 °C using a three electrode system and glass cell containing 200 mL of the prepared acid solutions at specific concentrations of ROV with Digi-Ivy 2311 potentiostat. Cylindrical LCS electrodes mounted in acrylic resin with an exposed surface area of 0.79 cm^2 were prepared. Polarization plots were obtained at a scan rate of 0.0015 V/s at potentials of -1.25 V and $+0.5$ V. Measured LCS steel coupons separately immersed in 200 mL of the dilute acid test solution for 240 h at 30 °C were weighed every 24 h to determine the corrosion rate from weight loss analysis. Images of corroded and inhibited LCS surface morphology from optical microscopy were analysed after weight-loss measurement with Omax trinocular through the aid of ToupCam analytical software. Spectral patterns of ROV/1 M HCl and H_2SO_4 solution (before and after the corrosion test) was evaluated and equated to the theoretical IR absorption table to identify the functional groups involved in the corrosion inhibition reactions after exposure to specific range of infrared ray beams from Bruker Alpha FTIR spectrometer between wavelengths of 375–7500 cm^{-1} and resolution of 0.9 cm^{-1}.

Results and Discussion

Potentiodynamic Polarization Studies

The potentiodynamic polarization curves of ROV reaction with LCS in HCl and H_2SO_4 acid solution are shown in Fig. 1a, b. Differences in corrosion rate for specimen A at 0% ROV and specimens B-G at 0.25–1.5% ROV is due to the intermolecular reaction of ROV inhibitor on LCS surface. Current peaks of the
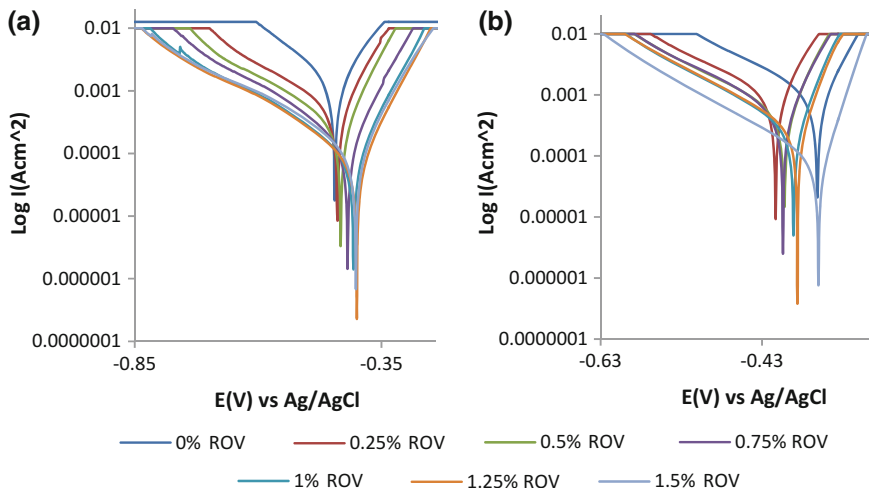
Fig. 1 Potentiodynamic polarization curves for LCS **a** 0–1.5% ROV in 1 M HCl, **b** 0–1.5% ROV in 1 M H_2SO_4

polarization curves in HCl solution (Fig. 1a) decreased significantly with increase in ROV concentration due to precipitation of ROV molecules which eventually shifts the polarization curves in the anodic direction. ROV has no effect on the cathodic Tafel slopes in comparison to anodic Tafel values. The anodic Tafel slope at 0% ROV is as a result of the formation of oxides due to slow electron transfer step (5, 6). Changes in Tafel slope values after 0% ROV is due to changes in the electrode substrate, rate controlling step and influence of potential controlled conditions, thus ROV altered the oxidation electrochemical reactions. LCS was subject to severe alloy degradation in H_2SO_4 solution at 0–0.75% ROV as shown in Fig. 1b. There was a significant improvement in corrosion rate values after 0.75% ROV due to increase in ROV molecules however the maximum inhibition efficiency attained is 60% due to the high current density at the intercept between the anodic and cathodic polarization curves, resulting from the debilitating action of SO_4^{2-}. There is a potential shift in the cathodic direction resulting from the release of excess electrons. After 0.5% ROV the potential shifts in the anodic direction till 1.5% ROV. The anodic Tafel slope values in H_2SO_4 tends to be lower than the values obtained in HCl show due to the strong electrocatalytic nature of LCS at high overpotentials in H_2SO_4.

Weight-Loss Measurement and Optical Microscopy Analysis

Figure 2a, b show the plot of LCS corrosion rate versus exposure time from the acid solutions. Macro images of LCS before corrosion and after corrosion, with and
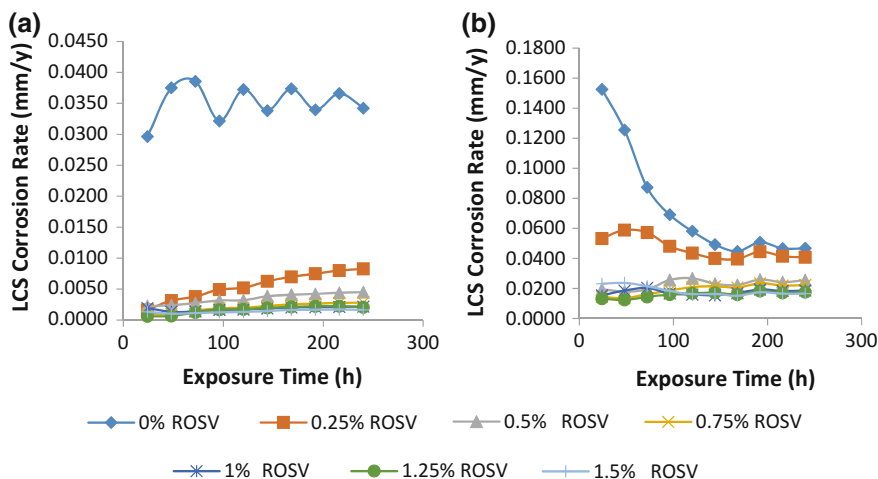
Fig. 2 Graphical illustration of **a** LCS corrosion rate versus exposure time in HCl, **b** LCS corrosion rate versus exposure time in H_2SO_4

without ROV are shown in Fig. 3a–c. Microscopic images of LCS before and after corrosion, with and without ROV are shown from Figs. 4a to 5b. LCS was subject to severe deterioration and corrosion in both acids at 0% ROV (Fig. 2a, b) resulting from the action of sulphates and chloride anions. This caused the formation of porous oxides on the steel (Fig. 3b, c). The corrosion rate at 0% ROV in H_2SO_4 decreased with respect to exposure time until steady state at 144–240 h; however the corrosion rate in HCl solution shifted continually at relatively higher values throughout due to the strong ionization potential of H_2SO_4. As a result of the inability of ROV molecules to effectively stall the surface deterioration of LCS in H_2SO_4 at lower ROV concentrations (Figs. 2a and 5a), transition from active deterioration of the steel surface to the passive state until 1–1.25% ROV. In HCl strong adsorption of ROV molecules after 0.25% ROV result in effective corrosion inhibition of LCS (Figs. 2b and 5b).

ATF-FTIR Spectroscopy Analysis

The spectra diagram (Fig. 6a) for ROV in HCl before corrosion test show peak configurations at wavelength with intensities of 3350.43, 2921.81, 2855.86, 2169.15, 1634.86 and 1458.03 cm^{-1} which refers to amines, amides, alcohols, phenols, alkanes, alkynes, aromatics and nitro compounds functional groups. Only the spectra peaks of 3331.26 and 1631.37 cm^{-1} remained after corrosion inhibition due to chemisorption adsorption of the functional groups at other peaks. The electrochemical action of ROV in H_2SO_4 (Fig. 6b) contrasts its behavior in HCl solution. The spectra peaks before corrosion test which consists of 3353,
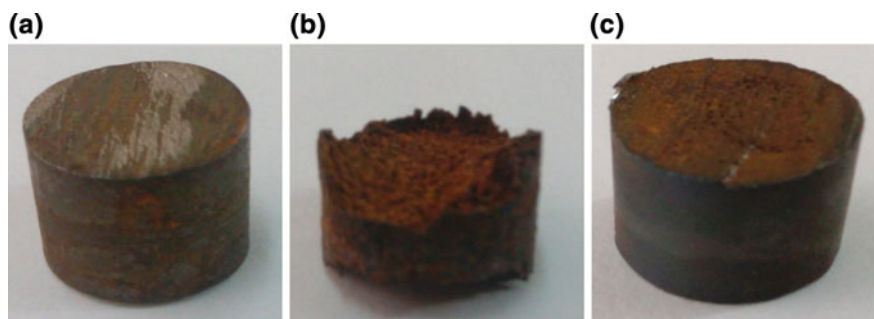
Fig. 3 Macro images of LCS **a** before corrosion, **b** after corrosion without ROV and **c** after corrosion with ROV
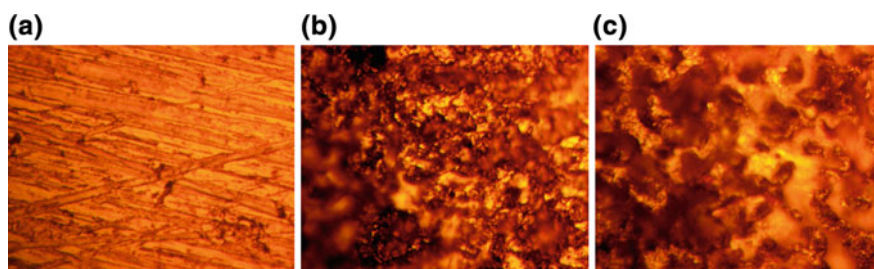
Fig. 4 Micro-analytical image of LCS **a** before corrosion, **b** after corrosion without ROV in HCl, **c** after corrosion without ROV in H_2SO_4
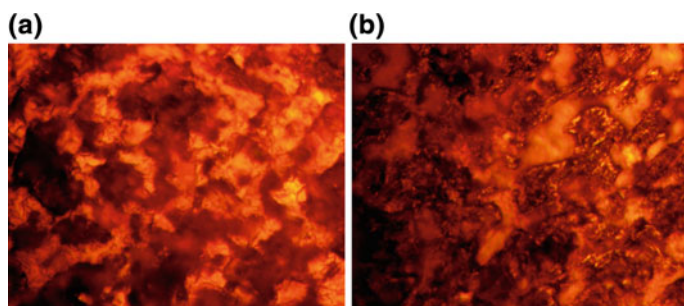
Fig. 5 Micro-analytical image of LCS after corrosion with ROV at mag. ×100 **a** in HCl, **b** in H_2SO_4

2954.05–2852.30, 1460.74, 1376.96, 1168.40, 1052.35 and 721 cm^{-1} (corresponding to alcohols, phenols, amines, amides, carboxylic acids, alkanes, aromatics, alkanes, alkanes, esters, ethers, alkyl halides and aliphatic amines) showed no
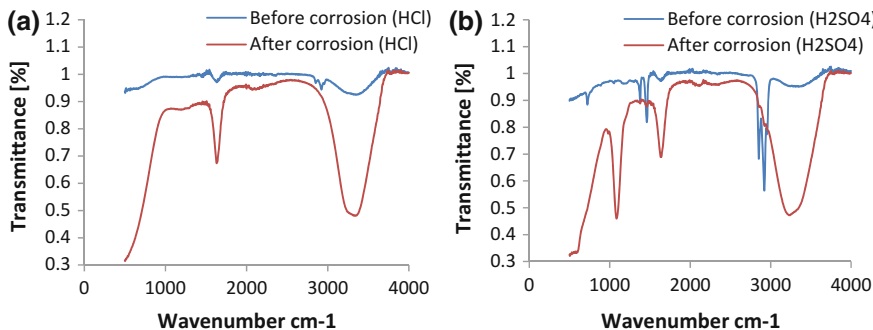
(a)

(b)

Fig. 6 ATF-FTIR spectra of ROV adsorption on LCS **a** 1 M HCl solution, **b** 1 M H_2SO_4

significant change in wavenumber but only decreased in peak intensity signifying limited adsorption of ROV on LCS.

Adsorption Isotherm

Electrochemical adsorption can be viewed as a replacement reaction of water molecules in the adsorbed layer by ROV molecules within the bulk acid solution. Langmuir, Freundlich and Temkin adsorption isotherm produced the best fit as shown from Figs. 7a to 9b. The plots of $\frac{C_{ROV}}{\theta}$ versus C_{ROV} for ROV adsorption in HCl showed linearity in agreement with Langmuir adsorption isotherm (Fig. 7a) with a correlation coefficient of 0.9999, In H_2SO_4 the plots (Fig. 7b) strongly deviated from ideal Langmuir model with a correlation coefficient of 0.3561. The plots for the Freundlich isotherm which states that adsorbed molecules interact and
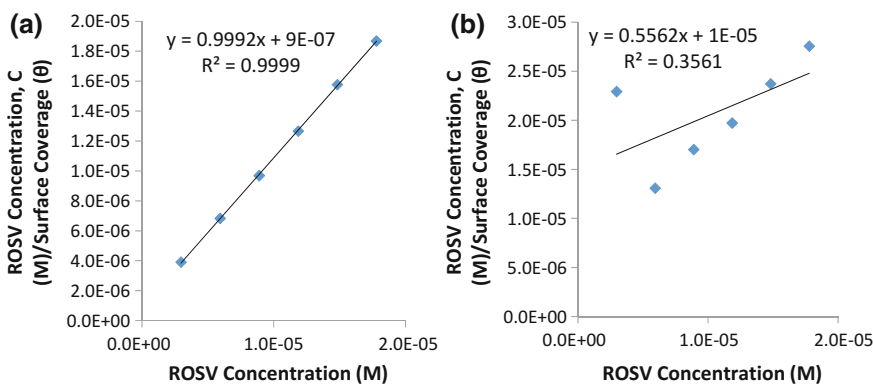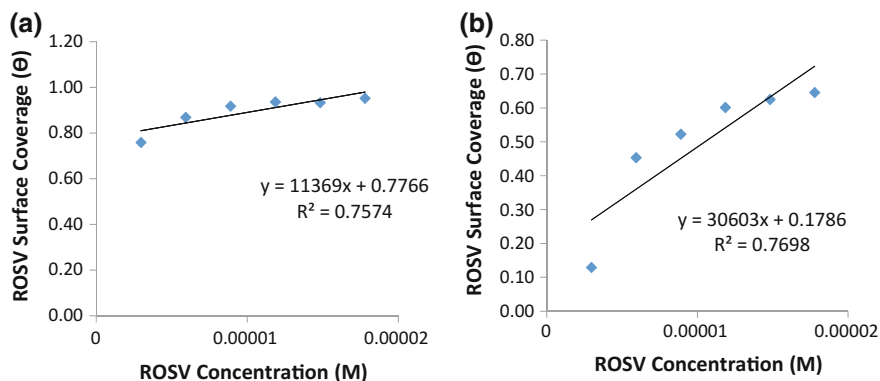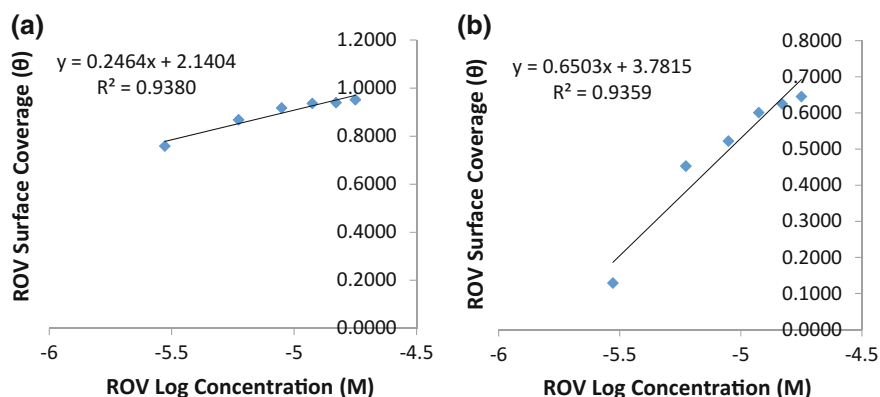
(a)

(b)

Fig. 7 Langmuir plot of $\frac{C}{\theta}$ versus ROV concentration in **a** 1 M HCl, **b** 1 M H_2SO_4

(a)

(b)

Fig. 8 Freundlich isotherm plot of ROV surface coverage (Θ) against ROV concentration **a** in HCl, **b** in 1 M H_2SO_4

(a)

(b)

Fig. 9 Temkin isotherm plot of ROV surface coverage (θ) against log ROSV concentration **a** in HCl, **b** in H_2SO_4

influence further adsorption through repulsion or attraction of molecules as the amount adsorbed is the total of adsorption on all sites (9, 10) showed a correlation coefficient of 0.7549 in HCl (Fig. 8a) and 0.7668 in H_2SO_4 (Fig. 8b). Temkin isotherm assumes the heat of adsorption decreases linearly with increase in surface coverage taking into account the indirect interactions of adsorbate-adsorbate molecules on adsorption isotherm. The Temkin isotherm plot for ROV in HCl (Fig. 9a) had a correlation coefficient of 0.9380 while in H_2SO_4 it is 0.9359 (Fig. 9b).

Thermodynamics of the Corrosion Process

The highest and lowest value of ΔG^{o}_{ads} in HCl is value obtained is -44.75 kJ mol^{-1} at 0.25% ROSV and -44.05 kJ mol^{-1} at 1.25% ROSV. These values align with chemisorption adsorption mechanism (12, 13). In H$_2$SO$_4$ the values are -39.31 kJ mol^{-1} at 0.5% ROSV and -36.77 kJ mol^{-1} at 0.25% ROSV which is consistent with physiochemical adsorption mechanism.

Conclusion

ROV compound effectively inhibited the corrosion of low carbon steel specimens studied in dilute molar concentrations of HCl acid solution but performed relatively poorly in H$_2$SO$_4$ acid due to the electrochemical action of sulphate anions. In HCl the compound chemically adsorbed onto the steel surface through the functional groups within its molecular structure, identified through ATF-FTIR spectroscopy analysis. Physiochemical interaction with the steel occurred in H$_2$SO$_4$ solution.